



HAL
open science

Variance-dependent neural activity in an involuntary averaging task

Rémy Allard, Stephen Ramanoël, Daphné Silvestre, Angelo Arleo

► **To cite this version:**

Rémy Allard, Stephen Ramanoël, Daphné Silvestre, Angelo Arleo. Variance-dependent neural activity in an involuntary averaging task. *Attention, Perception, and Psychophysics*, 2021, 10.3758/s13414-020-02223-8 . hal-03128096

HAL Id: hal-03128096

<https://hal.sorbonne-universite.fr/hal-03128096v1>

Submitted on 2 Feb 2021

HAL is a multi-disciplinary open access archive for the deposit and dissemination of scientific research documents, whether they are published or not. The documents may come from teaching and research institutions in France or abroad, or from public or private research centers.

L'archive ouverte pluridisciplinaire **HAL**, est destinée au dépôt et à la diffusion de documents scientifiques de niveau recherche, publiés ou non, émanant des établissements d'enseignement et de recherche français ou étrangers, des laboratoires publics ou privés.

1 Variance-dependent neural activity in an involuntary 2 averaging task

3 Rémy Allard^{1,2*}, Stephen Ramanoël^{1*}, Daphné Silvestre¹ & Angelo Arleo¹

4 ¹Sorbonne Universités, INSERM, CNRS, Institut de la Vision, 17 rue Moreau, F-75012 Paris,
5 France

6 ²School of optometry, Université de Montréal, Canada

7 <http://www.aging-vision-action.fr>

8 *These authors have contributed equally to this work

9 Corresponding author: Rémy Allard

10 Address: 3744 rue Jean-Brillant, local 260-7, Montreal, Quebec, Canada, H3T 1P1

11 Phone number: (514)343-6111 ext.8807

12 Email: remy.allard@umontreal.ca

13 Abstract

14 Ensemble statistics of a visual scene can be estimated to provide a gist of the scene without
15 detailed analysis of all individual items. The simplest and most widely studied ensemble
16 statistic is mean estimation, which requires averaging an ensemble of elements. Averaging is
17 useful to estimate the mean of an ensemble and discard the variance. The source of variance
18 can be external, i.e., variance across the physical elements, or internal, i.e., imprecisions in the
19 estimates of the elements by the visual system. The equivalent noise paradigm is often used to
20 measure the impact of the internal variance (i.e., the equivalent input noise). This paradigm
21 relies on the assumption that the averaging process is equally effective independently of the

22 main source of variance, internal or external, so any difference between the processing when
23 the main source of variance is internal and external must be assumed not to affect the averaging
24 efficiency. The current fMRI study compared the neural activity when the main variance is
25 caused by the stimulus (i.e., high variance) and when it is caused by imprecisions in the
26 estimates of the elements by the visual system (i.e., low variance). The results showed that the
27 right superior frontal and left middle frontal gyri can be significantly more activated when the
28 variance in the orientation of the Gabors was high than when it was low. Consequently, the use
29 of the equivalent noise paradigm requires the assumption that such additional neural activity in
30 high variance does not affect the averaging efficiency.

31 **Keywords**

32 Ensemble statistics; Averaging; Orientation; Noise; fMRI

33 **Introduction**

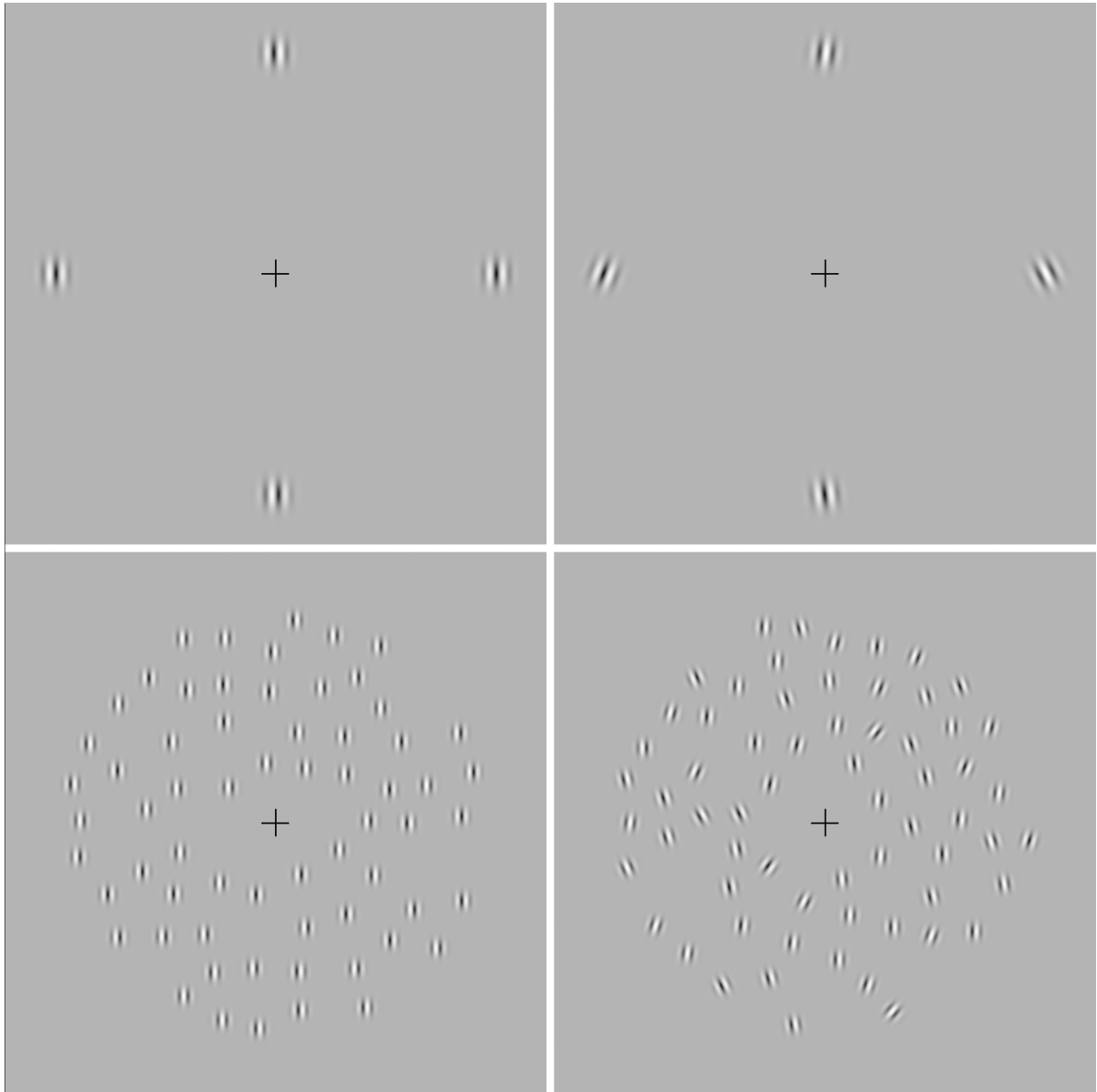
34 We have the subjective impression that we can perceive the entire visual scene at a glance, but
35 the visual system has limited resources and the entire visual scene cannot be simultaneously
36 processed with optimal efficiency. For instance, some processing requires the focus of attention
37 to be optimal, but attention can only be divided among few items (Pylyshyn & Storm, 1988;
38 Treisman & Gelade, 1980). Nevertheless, the visual system does not completely discard the
39 unattended information of the visual scene as some global information can be perceived even
40 in the absence of focal attention (for a review, see Whitney & Yamanashi Leib, 2018).
41 Ensemble statistics of a visual scene can be estimated to provide a gist of the visual scene
42 without detailed analysis of all individual items. The process of extracting ensemble statistics
43 is often described as “obligatory” or “compulsory” (Fischer & Whitney, 2011; Parkes, Lund,
44 Angelucci, Solomon, & Morgan, 2001) as attention may not necessarily be required (Alvarez
45 & Oliva, 2008, 2009; Bronfman, Brezis, Jacobson, & Usher, 2014; Chong & Treisman, 2005).
46 The simplest and most widely studied ensemble statistic is mean estimation, which requires
47 averaging an ensemble of elements. Averaging is useful to estimate the mean of an ensemble
48 and discard the variance. When the variance across elements is high, the ability to estimate the
49 mean of the a priori distribution (e.g., orientation discrimination threshold) depends on the
50 averaging efficiency (also referred to as calculation efficiency or sampling efficiency), which
51 quantifies the observer’s performance relative to the ideal performance (e.g., Beaudot &
52 Mullen, 2006). Since the correctness of the answer is defined relative to the mean of the a priori
53 distribution, the ideal performance is limited by the variance of the a priori distribution.
54 When the variance is low (e.g., all identical elements), the performance of a human observer
55 cannot solely depend on the averaging efficiency as performance is also limited by imprecisions
56 in the estimates of the elements (i.e., internal noise) by the visual system. Consequently, in

57 absence of external variance, the ability to estimate the mean of the a priori distribution is
58 typically presumed to depend on two factors (Beaudot & Mullen, 2006; Dakin, 2001, 2015;
59 Dakin, Bex, Cass, & Watt, 2009; Dakin, Mareschal, & Bex, 2005; Mansouri, Allen, Hess,
60 Dakin, & Ehrt, 2004; Mareschal, Bex, & Dakin, 2008; Tibber et al., 2015): the variance
61 introduced by the visual system (typically referred to as internal noise) and the averaging
62 efficiency of the effective stimulus (i.e., the stimulus + orientation-jitter due to imprecisions in
63 samples estimates). The equivalent noise paradigm is often used to evaluate the impact of these
64 imprecisions. Knowing the performance in absence of noise and the effective averaging
65 efficiency in absence of noise enables to derive the internal variance due to imprecisions in
66 samples estimates. However, the effective averaging efficiency in absence of noise cannot be
67 directly measured. Nevertheless, by assuming (usually implicitly) that the effective averaging
68 efficiency in absence of noise is the same as the averaging efficiency measured in high noise
69 (i.e., the noise-invariant processing assumption, Allard & Cavanagh, 2011; or the contrast-
70 invariant calculation assumption Pelli, 1990), it is possible to derive the internal variance based
71 on the performance in absence of noise and in high noise. Consequently, this assumption is
72 critical for evaluating the internal noise using the equivalent noise paradigm.

73 The equivalent noise paradigm is more commonly used for contrast thresholds and white pixel
74 noise, and relies on the noise-invariant processing assumption (Allard & Cavanagh, 2011, 2012;
75 or the contrast-invariant processing assumption, Pelli, 1990): the calculation efficiency
76 measured in high noise is assumed to be the same as the effective calculation efficiency in low
77 noise. The presence of high white pixel noise obviously increases neural activity, so to use the
78 equivalent noise paradigm, one must assume that this additional neural activity in high noise
79 does not affect the calculation efficiency. This assumption has been criticized by Baker and
80 colleagues (Baker & Meese, 2012; Baker & Vilidaite, 2014; Baldwin, Baker, & Hess, 2016),
81 who argue that white noise may compromise the use of the equivalent because it introduces

82 neural activity that can interfere with the processing of the target (but see Allard & Faubert,
83 2013, 2014). Although it is obvious that some neural activity is greater in the presence of white
84 pixel noise than the absence of noise due to the greater contrast, it is not obvious if adding
85 increasing the variance across elements would increase neural activity. For instance, we would
86 not necessarily expect additional neural activity when adding an orientation jitter to each
87 element of an ensemble.

88 An important distinction that is not always explicitly stated is that the averaging process can be
89 voluntary or involuntary (Dakin et al., 2009). For voluntary averaging, only a small number of
90 elements is presented (e.g., 4, Allard & Cavanagh, 2012; or 6, Dakin et al., 2009), each element
91 is perceptually distinct (e.g., top row in Figure 1), and the observer voluntarily decides to
92 estimate the mean of an attribute (e.g., orientation) or not. The triggering of this averaging
93 process therefore depends on the volition of the observer so it is not compulsory or obligatory.
94 For involuntary averaging, however, computing the mean is compulsory or obligatory, that is,
95 beyond the volition of the observer (Dakin et al., 2009; Fischer & Whitney, 2011; Parkes et al.,
96 2001). Involuntary averaging typically occurs when a large amount of elements are presented
97 in the periphery (e.g., bottom row in Figure 1) and is particularly relevant for scene perception
98 as it provides a gist of the ensemble statistics and has been studied for many attributes such as
99 orientation (e.g., Alvarez & Oliva, 2009), size (Im & Halberda, 2013), motion (Mareschal et
100 al., 2008) and color (Bronfman et al., 2014).



101

102 **Figure 1. Examples of stimuli for the voluntary (top) and involuntary (bottom) for low (left) or high (right)**
103 **variance across samples. The task consisted in judging the mean orientation of the ensemble relative to**
104 **vertical (clockwise or counterclockwise).**

105 For voluntary averaging (e.g., top row in Figure 1), Allard and Cavanagh (2012) concluded that
106 observers averaged the physical (i.e., external) variance across elements, but not the internal
107 variance resulting from imprecision estimates of individual elements by the visual system. In
108 other words, they voluntarily and effectively averaged dissimilar elements, but not apparently
109 identical elements. This claim was based on the psychophysical finding that performance at

110 discriminating the mean of the a priori distribution improved with the number of samples in
111 high variance (i.e., high jitter added to every elements), but not in low variance (i.e., identical,
112 or nearly identical, elements and variance in sample estimates is mainly due to the sample
113 estimates by the observers). They concluded that some voluntary averaging processing
114 operating in high variance was not effective in low variance, which contradicts the noise-
115 invariant processing assumption (Allard & Cavanagh, 2011; in the current context, it could also
116 be referred to as the “variance-invariant processing assumption”) that the same processing
117 operates in low and high variance. However, it has been argued that the result of this
118 psychophysical study does not necessarily imply different averaging efficiencies in low and
119 high variance as the apparent absence of averaging efficiency in low variance could be
120 explained by greater imprecision estimates with more samples (Dakin, 2015) or by
121 multiplicative noise (i.e., internal variance proportional to the external variance, Bocheva,
122 Stefanov, Stefanova, & Genova, 2015). Thus, despite the observable voluntary averaging
123 efficiency in high variance and the absence of observable efficiency in low variance, the claim
124 that different averaging processes operate in both conditions (i.e., the variance-invariant
125 processing assumption underlying the equivalent noise paradigm) remains debated.

126 Given that voluntary averaging depends on the volition of the observer, a variance-dependent
127 averaging process would not be surprising; why bother voluntarily averaging elements that
128 appear identical? On the other hand, we may intuitively expect involuntary averaging
129 processing to be independent of the variance across the elements to average. Indeed, a
130 compulsory or obligatory averaging process would be expected to operate whether the
131 perceived variance across elements is mainly due to the stimulus variance across elements when
132 the variance is high or to imprecisions in the estimates of the samples when the variance is low
133 (e.g., identical samples).

134 The aim of the current study was to investigate if the processing differs whether the main source
135 of the sample imprecision is coming from the stimulus (i.e., high variance) or from the
136 imprecision estimates of the observer (i.e., low variance). For this purpose, we recorded the
137 neural activity when the main variance was coming from the stimulus and from the observer
138 for a voluntary (i.e., 4 sparse elements; top images in Figure 1) and an involuntary (64 elements
139 presented in the periphery; bottom images in Figure 1) orientation-averaging task.

140 **Method**

141 ***Participants***

142 Seventeen young adults were included in the study (9 females; mean age \pm SD: 26.6 ± 4.4
143 years; age range: 21-38 years), but 3 subjects were excluded for in-scanner motion
144 (movements > 3 mm across trials). The participants were part of the French cohort population
145 SilverSight (~350 subjects) established and followed-up ever since 2015 at Vision Institute –
146 Quinze-Vingts National Ophthalmology Hospital, Paris, France (Lagrené et al., 2019). All
147 participants were right-handed, had normal or corrected-to-normal vision, and they had no
148 history of neurological or psychiatric disorders, or ocular disorders, or sensorimotor
149 dysfunctions. All participants gave their informed written consent before participating in the
150 study in accordance with the tenets of the Declaration of Helsinki and they were approved by
151 the Ethical Committee “CPP Ile de France V” (ID_RCB 2015-A01094-45, CPP N°: 16122).

152 ***Apparatus***

153 Stimuli were displayed using nordicAktiva software (<https://www.nordicneurolab.com/>) on an
154 MRI-compatible liquid crystal display monitor (NordicNeuroLab, Bergen, Norway) positioned
155 at the head of the scanner bore. Participants viewed the screen (size: 69.84 cm (H) x 39.26 cm
156 (V); pixels: 1920 x 1080; refresh rate: 120 Hz, mean luminance intensity: 203 cd/m²) at a

157 distance of 115 cm via a mirror fixed above the head-coil. The visible part of the screen
158 subtended approximately 34 x 19 degrees of visual angle (dva).

159 ***Stimuli and Procedure***

160 Observers were asked to report the mean orientation of an ensemble of Gabors relative to
161 vertical and respond as soon as possible, while answering as accurately as possible. For
162 voluntary averaging, the stimuli were similar to the ones of a previous study on voluntary
163 averaging (Allard & Cavanagh, 2012): 4 Gabors displayed 8 dva to the left, right, above, and
164 below fixation (top row in Figure 1) so that each element was perceptually distinct (Dakin et
165 al., 2009). The spatial frequency of the Gabors was 2 cpd; their spatial envelope was a Gaussian
166 with a SD of 0.33 dva; their contrast was maximized and their phases were randomized.

167 For involuntary averaging, 64 Gabors were presented in the periphery in which case computing
168 their mean orientation is expected to be compulsory or obligatory, that is, beyond the volition
169 of the observer (Dakin et al., 2009; Fischer & Whitney, 2011; Parkes et al., 2001). The Gabors
170 were randomly positioned between 2 and 8 dva of eccentricity with the constraint that center-
171 to-center distance between Gabors had to be at least 1.5 dva (bottom row in Figure 1). In order
172 to increase the gap between Gabors, their Gaussian spatial envelope was smaller (SD of 0.17
173 dva) and their spatial frequency was 3 cpd.; their contrast was maximized and their phases were
174 randomized.

175 In the low variance condition, the Gabors were all vertically orientated. In the high variance
176 condition, the orientations of the Gabors were selected from a Gaussian distribution centered
177 vertically with a SD of the distribution of 16 degrees. The stimuli were presented for 200 ms,
178 which was too brief for the observer to saccade to the target (Hallett, 1986).

179 We used a block-design paradigm with 4 different conditions: low-variance with 4 elements
180 (LV-4; top-left in Figure 1), low-variance with 64 elements (LV-64; bottom-left in Figure 1),

181 high-variance with 4 elements (HV-4; top-right in Figure 1) and high-variance with 64
182 elements (HV-64; bottom-right in Figure 1). 120 trials were performed per condition for a
183 total of 480 trials. These trials were separated among six functional runs presented in a
184 random order: 3 runs for voluntary averaging (LV-4 and HV-4), and 3 runs for involuntary
185 averaging (LV-64 and HV-64). Each functional scan lasted 5 minutes and was composed of
186 sixteen 5-trial blocks alternating between LV and HV with the first block randomly selected
187 (LV or HV). Each 5-trial block lasted 15 seconds. The sixteen blocks were interspersed with
188 four 15-second blocks with a fixation cross at the center of the screen (Fixation condition)
189 displayed against a gray background.

190 Each stimulus was displayed for 200 ms followed by a fixation cross in the center of the
191 screen displayed against a gray background. The interval between the onset of two successive
192 stimuli was 2.8 s. Participants had to give a categorical answer after each image by pressing
193 the corresponding handheld grips response device (NordicNeurolab) to indicate whether the
194 mean orientation of the Gabors was tilted clockwise or counterclockwise from vertical. They
195 were instructed to fixate on the center of the screen (fixation cross) during the entire
196 experiment and to respond as accurately and as quickly as possible. Response accuracy and
197 reaction times were recorded.

198 A practice session in a psychophysical laboratory was conducted a few days before the
199 experiment for participants to be familiarized with the psychophysical task and the four types
200 of stimuli prior to the data acquisition.

201 ***fMRI acquisition***

202 Images were acquired using a 3T Siemens Magnetom Skyra whole-body MRI system
203 (Siemens Medical Solutions, Erlangen, Germany) with a 64-channel head-coil at the Quinze-
204 Vingts National Ophthalmology Hospital in Paris, France. Task-based fMRI and an

205 anatomical image were acquired for all participants. The anatomical volume consisted of a
206 T1-weighted, high-resolution, three-dimensional MPRAGE sequence (TR/TE/IT/flip angle =
207 2300 ms/ 2.9 ms/ 900 ms/ 9°; matrix size = 256 x 240 x 176; voxel size = 1 x 1 x 1.2 mm).
208 For functional scan, 304 volumes of 64 slices were acquired using a T2*-weighted SMS-EPI
209 sequence (TR/TE/flip angle = 1000 ms/ 30 ms/ 90°; matrix size = 100 x 100; SMS = 2;
210 GRAPPA = 2; voxel size = 2.5 x 2.5 x 2.4 mm).

211 ***Data analysis***

212 Data analysis was performed using SPM12 release 7487 (Wellcome Department of Imaging
213 Neuroscience, London, UK, www.fil.ion.ucl.ac.uk/spm) implemented in MATLAB 2018a
214 (Mathworks Inc., Natick, MA, USA).

215 For each participant, the first 4 functional volumes of each runs were discarded to allow for
216 equilibration effects. The remaining volumes were realigned to correct for head movements to
217 the mean functional images using a rigid body transformation. The T1-weighted anatomical
218 volume was then realigned (affine transformation) to match the mean functional image of
219 each participant, and was then normalized (non-rigid, non-linear transformation) into the MNI
220 space. A 4th degree B-Spline interpolation was applied. The anatomical normalization
221 parameters were subsequently used for the normalization of functional volumes. Finally, each
222 functional scan was smoothed by an 8 mm FWHM (Full Width at Half Maximum) Gaussian
223 kernel. Slice-timing correction was not applied in line with the recommendations of the
224 Human Connectome Project functional preprocessing pipeline for multi-slice sequences
225 (Glasser et al., 2013).

226 Statistical analysis was performed using general linear model (Friston et al., 1994) for block
227 designs at single participant level. For each participant, five conditions of interest (LV-4, LV-
228 64, HV-4, HV-64 and Fixation) were modelled as five regressors, constructed as box-car

229 functions and convolved with a canonical hemodynamic response function. Reaction-time for
230 each trial and movement parameters derived from realignment corrections (three translations
231 and three rotations) were also considered in the model as an additional factor of no interest to
232 account for related variance. Time-series for each voxel were high-pass-filtered (1/128 Hz
233 cutoff) to remove low-frequency noise and signal drift. On an individual level (first level
234 analysis), we identified the brain regions involved in the processing of each level of variance
235 content relative to the fixation ([LV-ALL > Fixation], and [HV-ALL > Fixation]) irrespective
236 to the number of elements. Then, we identified the cerebral regions involved in the processing
237 of low-variance stimuli related to the high-variance stimuli, as well as the inverse fMRI
238 contrast ([LV-ALL > HV-ALL] and, [HV-ALL > LV-ALL]). We also, tested the effect of
239 number of elements ([ALL-4 > ALL-64], and [ALL-64 > ALL-4]) irrespective to the variance
240 content, and we identified brain regions involved in the processing of variance related to the
241 number of elements ([LV-4 > HV-4], [HV-4 > LV-4], [LV-64 > HV-64], and [HV-64 > LV-
242 64]). Finally, we tested the effect of level of variance for both number of elements conditions
243 relative to the fixation ([LV-4 > Fixation], [HV-4 > Fixation], [LV-64 > Fixation], and [HV-
244 64 > Fixation]).

245 To allow population inference, we performed a second level-random analysis using a one-
246 sample t-test. Areas of activation were considered significant if they exceed a significant
247 threshold fixed at $p < 0.05$ FWE-corrected for multiple comparisons at cluster level, with a
248 minimum cluster extend $k=20$.

249 **Results**

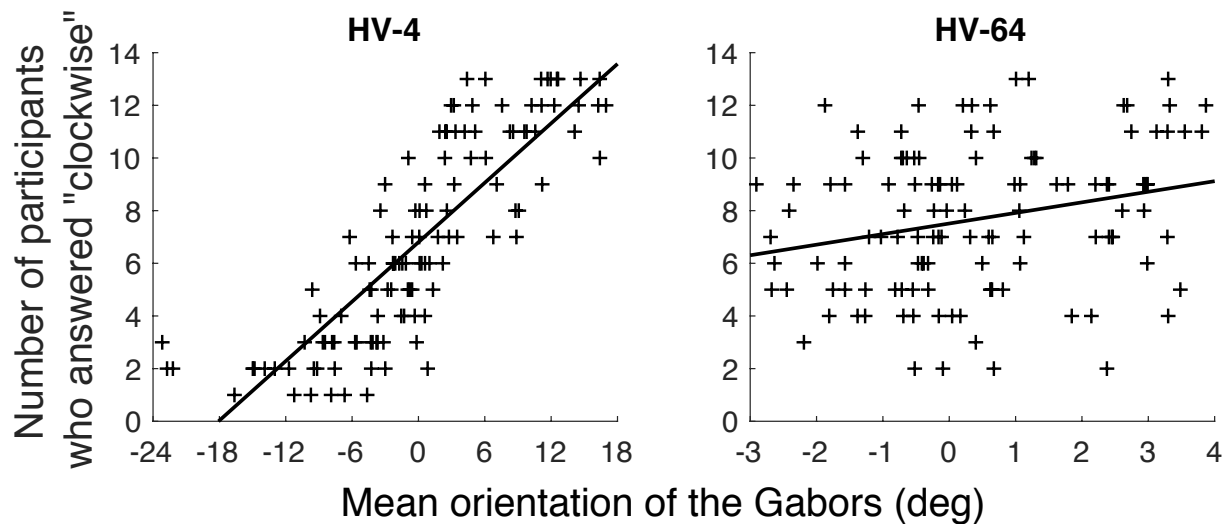
250 ***Behavior***

251 The percentage of trials on which participants did not give an answer within 2.8 seconds was
252 lower than 1% for each of the four conditions (LV-4=0.6%; HV-4=0.8%; LV-64=0.5% and

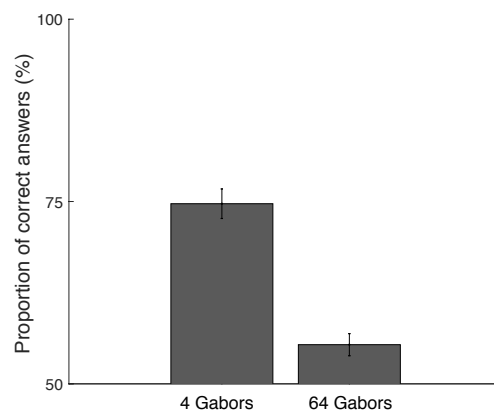
253 HV-64=0.5%). These results confirm that participants followed the instructions to respond as
254 fast as possible. No-response trials were removed from behavioral analyses.

255 Figure 2 shows the number of participants who answered clockwise for each stimulus as a
256 function of the mean of the ensemble for conditions in high variance. With 4 Gabors (left
257 graph in Figure 2), the mean orientation of the stimulus varied considerably across stimuli and
258 the participants' answers were highly correlated with the stimulus' mean orientation as
259 confirmed by a linear regression analysis ($b=0.38$, $t(11)=16.7$, $p<0.001$). Indeed, when the
260 mean orientation was highly tilted clockwise, almost all of participants answered "clockwise"
261 and when the mean orientation was highly tilted counterclockwise, almost all of them
262 answered "counterclockwise" (i.e., just a few answered "clockwise"). As a result, the
263 participants' answers were stimulus driven, not random (Figure 3). With 64 Gabors (right
264 graph in Figure 2), the stimulus' mean orientation was much closer to vertical due to the
265 greater number of elements. Although the participants' answers were less correlated with the
266 actual stimulus mean (Figure 3), the participants' answers also significantly depended on the
267 mean orientation ($b=0.40$, $t(11)=2.93$, $p<0.01$). These results confirm that participants
268 effectively performed the task of reporting the mean orientation relative to vertical (i.e., they
269 did not answer randomly).

270



271
 272 **Figure 2. Number of participants who answered “clockwise” as a function of the mean of the ensemble for**
 273 **each of the 120 stimuli in high variance with 4 Gabors (HV-4, left) and with 64 Gabors (HV-64, right).**
 274 **The solid lines represent the linear regressions.**

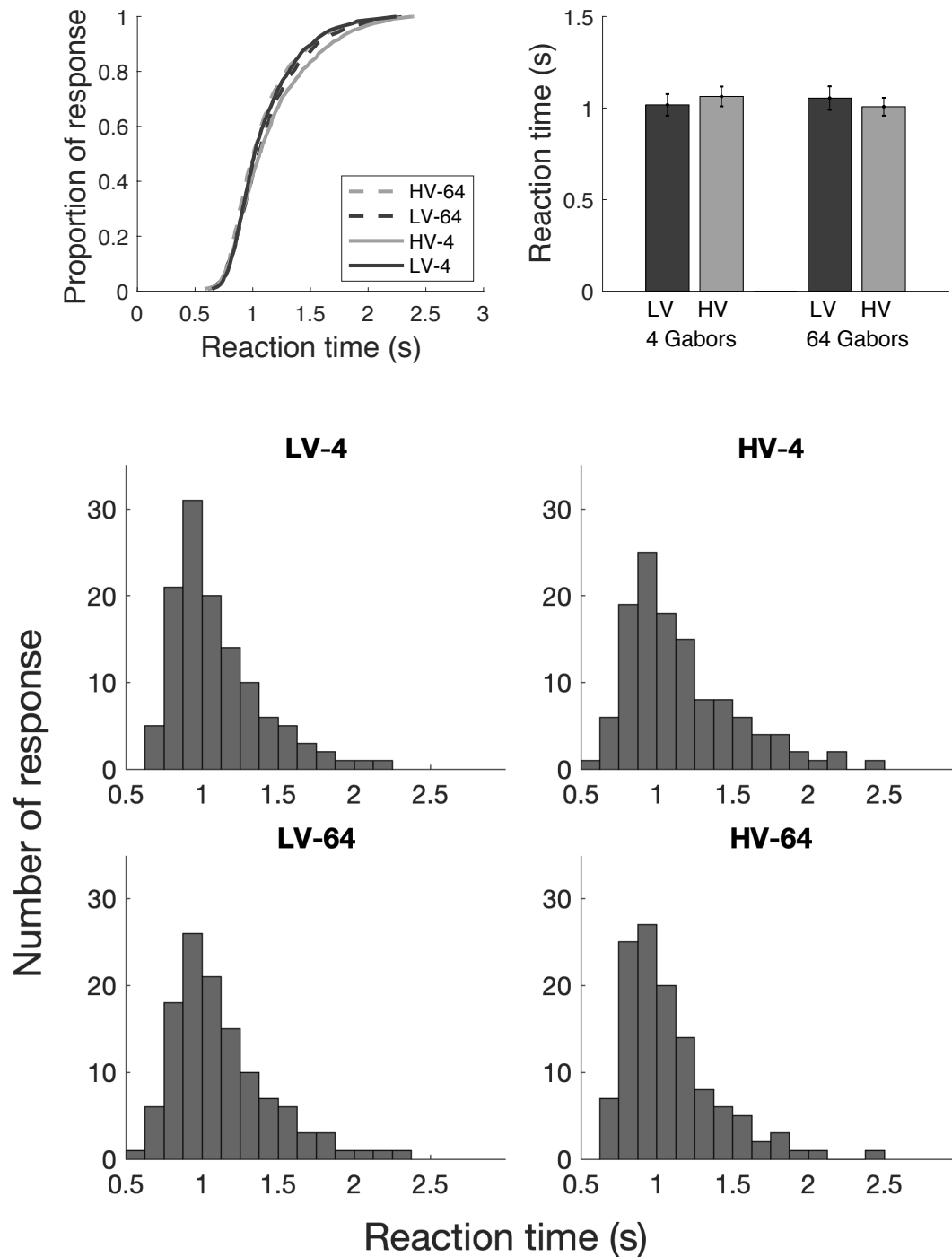


275
 276 **Figure 3. Proportion of correct answers for both tasks in high variance. Error bars represent standard**
 277 **error from the mean.**

278 The distributions for the reaction times and the median reaction times (Figure 4) were highly
 279 similar for the 4 conditions. The reaction times for the 4 conditions were analyzed with an
 280 inverse Gaussian generalized linear mixed model with an identity link and no significant
 281 effect was found for the two fixed factors, which were the variance (estimate=12.15 , $t= 1.25$,
 282 $p=0.21$) and the number of elements (estimate=-0.26 , $t= -1.58$, $p=0.11$). The fact that similar
 283 reaction times were observed in low and high variance is compatible with the hypothesis that
 284 the processing was independent of the variance across elements (i.e., the variance-invariant

285 processing assumption). Consequently, from the behavioral data alone, there was no evidence
 286 of different processing involved in low and high variance (but see fMRI results below).

287



288

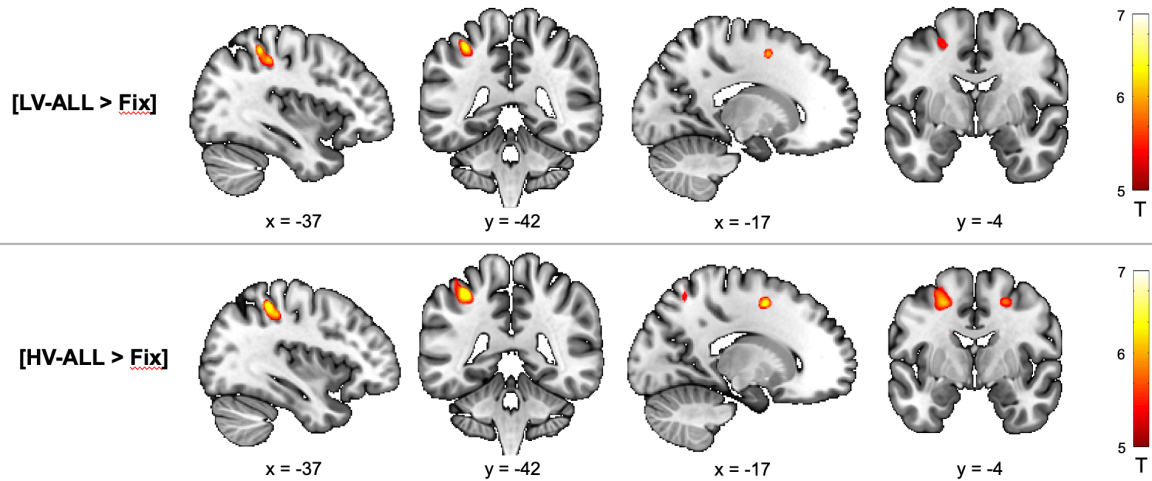
289 **Figure 4. Proportion of response given as a function of the reaction time for the four conditions with all**
 290 **the participants (top left). Mean median reaction times for the four conditions averaged across observers**
 291 **(top right). LV = low variance condition and HV = high variance condition. Error bars represent standard**
 292 **error from the mean. Histograms of the reaction times for the 4 conditions (bottom).**

293 **fMRI**

294 *Effect of variance content.* Results for the effect of variance content relative to the fixation,
 295 irrespective to the number of elements are shown in Table 1 and Figure 5. Results for direct
 296 comparisons of variance conditions are presented in Table 2 and Figure 6.

fMRI contrasts		H	BA	k	x	y	z	t
[LV-ALL > Fix]	Superior Parietal Gyrus	L	7	94	-35	-42	53	9.16
	[Postcentral Gyrus]		1		-40	-35	48	7.10
	Superior Frontal Gyrus	L	6	49	-17	1	50	6.81
[HV-ALL > Fix]	Superior Parietal Gyrus	L	7	141	-35	-42	53	11.22
					-40	-35	48	8.40
					-42	-40	58	6.65
	Superior Frontal Gyrus	L	6	191	-17	3	53	7.54
	[Middle Frontal Gyrus]				-30	1	60	7.54
	[Middle Frontal Gyrus]				-25	-5	50	6.85
	Middle Frontal Gyrus	R	6	36	26	-2	53	6.40

297 **Table 1. Cerebral regions exhibiting an effect of the level of variance (low-variance stimuli: LV-ALL and**
 298 **high-variance stimuli: HV-ALL) related to fixation (Fix). The statistical threshold for cluster was defined**
 299 **as $p < 0.05$ FWE corrected for multiple comparisons with an extent voxel threshold defined as 20 voxels.**
 300 **Only regions revealing significant differences between conditions were included. For each cluster, the**
 301 **region showing the maximum t-value was listed first, followed by the other regions in the cluster [in**
 302 **square brackets]. Montreal Neurological Institute (MNI) coordinates (x, y, z) of the peak and number of**
 303 **voxels (k) of clusters are also shown. H = hemisphere; R = right hemisphere; L = left hemisphere; BA =**
 304 **Brodman area.**



305

306

307

308

Figure 5. Cerebral regions whose activity was elicited by the fMRI contrasts [LV-ALL > Fix] and [HV-ALL > Fix] projected onto 2D slices ($p < 0.05$ FWE-corrected at cluster level, $k=20$; LV = low-variance; HV = high-variance; Fix = fixation).

		H	BA	k	x	y	z	t
fMRI contrasts								
[LV-ALL > HV-ALL]	<i>No significant activation</i>							
[HV-ALL > LV-ALL]	Cerebellum	L	-	59	-30	-75	-30	6.22
	[Inferior Occipital Gyrus]			19	-40	-77	-18	6.07
	Middle Frontal Gyrus	L	6	37	-35	6	38	6.33
	[Middle Frontal Gyrus]				-30	-16	38	5.79

309

310

311

312

313

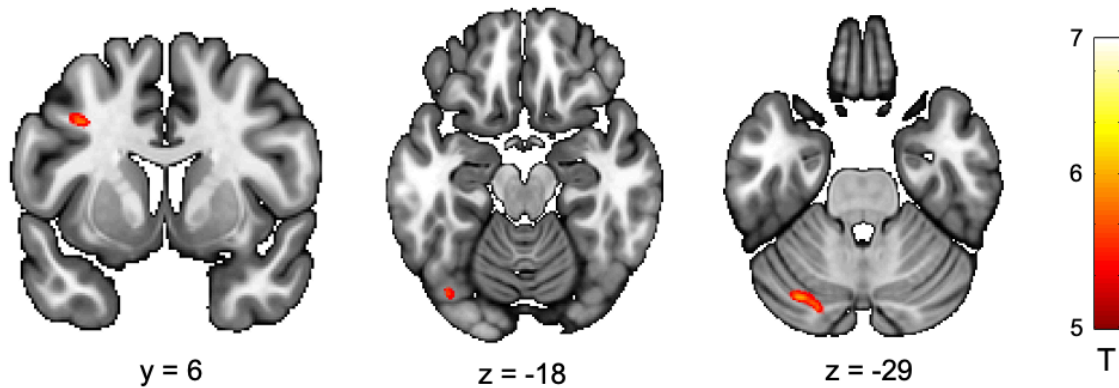
314

315

316

Table 2. Cerebral regions exhibiting an effect for direct comparison of variance contents between low-variance (LV-ALL) and high-variance (HV-ALL) stimuli. The statistical threshold for cluster was defined as $p < 0.05$ FWE corrected for multiple comparisons with an extent voxel threshold defined as 20 voxels. Only regions revealing significant differences between conditions were included. For each cluster, the region showing the maximum t-value was listed first, followed by the other regions in the cluster [in square brackets]. Montreal Neurological Institute (MNI) coordinates (x, y, z) of the peak and number of voxels (k) of clusters are also shown. H = hemisphere; R = right hemisphere; L = left hemisphere; BA = Brodmann area.

[HV-ALL > LV-ALL]



317

318 **Figure 6. Cerebral regions whose activity was elicited by the fMRI contrast [HV-ALL > LV-ALL]**
319 **projected onto 2D slices ($p < 0.05$ FWE-corrected at cluster level, $k=20$; LV = low variance, HV = high**
320 **variance).**

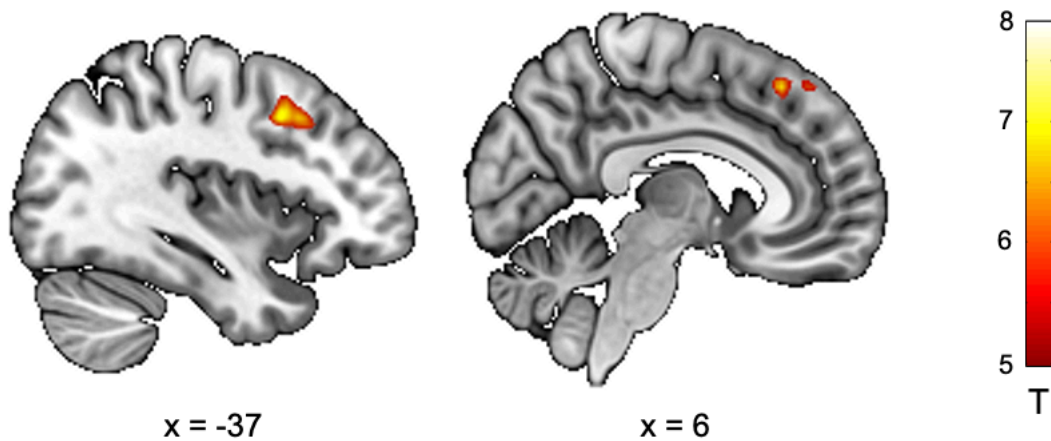
321 We began by contrasting the processing of Gabor orientation in low-variance to fixation
322 ([LV-ALL > Fix] contrast), and observed recruitment of the superior parietal and the superior
323 frontal gyri in the left hemisphere. Similarly, the processing of Gabor orientation in high-
324 variance condition ([HV-ALL > Fix]) showed activation of the superior parts of the parietal
325 and frontal gyri in the left hemisphere, and supplementary involvement of the middle frontal
326 gyrus bilaterally. Direct comparisons of variance contents showed no significant results for
327 low-variance to high-variance ([LV-ALL > HV-ALL]). The opposite contrast ([HV-ALL >
328 LV-ALL]) elicited activations in the cerebellum, the inferior occipital gyrus and the middle
329 frontal gyrus in the left hemisphere.

330 Critically, the direct comparison of variance conditions related to the number of elements
331 showed significant results only for the contrast [HV-64 > LV-64] involving the recruitment of
332 the left middle frontal gyrus and the superior frontal gyrus bilaterally (mainly in the right
333 hemisphere; see Table 3 and Figure 7).

fMRI contrasts		H	BA	k	x	y	z	t
[LV-4 > HV-4]	<i>No significant activation</i>							
[HV-4 > LV-4]	<i>No significant activation</i>							
[LV-64 > HV-64]	<i>No significant activation</i>							
[HV-64 > LV-64]	Middle Frontal Gyrus	L	8	93	-37	11	40	7.43
	Superior Frontal Gyrus	R	8	33	6	31	50	6.89
[LV-4 > HV-64]	<i>No significant activation</i>							
[HV-64 > LV-4]	<i>No significant activation</i>							
[LV-64 > HV-4]	<i>No significant activation</i>							
[HV-4 > LV-64]	<i>No significant activation</i>							

334 **Table 3. Cerebral regions exhibiting an effect for direct comparisons between variances conditions related**
335 **to the number of elements (low-variance with 4 elements: LV-4, high-variance with 4 elements: HV-4,**
336 **low-variance with 64 elements: LV-64 and high-variance with 64 elements: HV-64) related to fixation**
337 **(Fix). The statistical threshold for cluster was defined as $p < 0.05$ FWE corrected for multiple comparisons**
338 **with an extent voxel threshold defined as 20 voxels. Only regions revealing significant differences between**
339 **conditions were included. Montreal Neurological Institute (MNI) coordinates (x, y, z) of the peak and**
340 **number of voxels (k) of clusters are also shown. H = hemisphere; R = right hemisphere; L = left**
341 **hemisphere; BA = Brodmann area.**

[HV-64 > LV-64]



342

343 **Figure 7. Cerebral regions whose activity was elicited by the fMRI contrast [HV-64 > LV-64] projected**
344 **onto 2D slices ($p < 0.05$ FWE-corrected at cluster level, $k=20$; LV = low-variance, HV = high-variance).**

345 *Effect of number of elements.* Direct comparisons of the number of elements irrespective to
346 the variance contents for Gabor orientations ([ALL-4 > ALL-64], and [ALL-64 > ALL-4]
347 showed no significant results. Results for the effect of the number of elements related to the
348 variance contents compared to the fixation condition are shown in supplementary information
349 section (SI-Table 1 and SI-Figure 1).

350 Results for the processing of variance contents related to the number of elements relative to
351 the fixation showed activation for high variance only for 4 Gabors and for both low- and high-
352 variances conditions for 64 Gabors. Precisely, these three contrasts ([HV-4 > Fix], [LV-64 >
353 Fix], and [HV-64 > Fixation]), involved common cerebral structures with the left superior
354 parietal gyrus, the left middle and superior frontal gyri. In addition, the contrast [HV-4 > Fix]
355 elicited specific activation of the middle and superior frontal gyri in the right hemisphere
356 whereas the contrast [LV-64 > Fix] elicited activation located in the left supramarginal gyrus.
357 Finally, the contrast [HV-64 > Fix] showed significant results also on the left supramarginal
358 gyrus and the right middle occipital gyrus.

359 **Discussion**

360 The reaction times around 1 second are consistent with a previous study (Bocheva et al., 2015)
361 in which participants were also asked to respond as fast as possible (while being accurate). The
362 fact that the reaction times in the current study did not vary with the variance across samples
363 (i.e., between LV and HV) is consistent with the variance-invariant processing assumption: in
364 low variance, imprecisions in sample estimates introduces variance across samples and the
365 observer averages these estimates as they do in high variance. These results diverge from the
366 ones of Bocheva and colleagues, who found reaction times longer with higher variance stimuli,
367 but can be explained by the task difficulty. In Bocheva's study, the same signal strengths (i.e.,
368 mean of the a priori distribution) were used at all variances, but mean orientation discrimination
369 thresholds were higher with higher variance, so the task was, on average, more difficult at
370 higher variance (lower signal strength relative to the participants' thresholds). In the current
371 study, all conditions were below thresholds as the mean of the a priori distribution was 0 (note
372 that according to the equivalent noise paradigm, the correctness must be defined relative to the
373 mean of the a priori distribution, not the actual mean of the stimulus). Thus, without a signal
374 strength greater relative to threshold, we did not observe in the behavioral data a violation of
375 the variance-invariant processing assumption, that is, that the same averaging processing
376 operates independently of the source of the main variance (imprecisions in sample estimates or
377 the stimulus). Conversely, the results regarding the response time suggests that the different
378 reaction times observed at different levels of variance in a previous study was due to a
379 confounding factor (i.e., task difficulty), not variance level per se.

380 The fMRI data showed that low- and high-variance elicited neural activations within common
381 brain regions including the superior parietal and frontal gyri in the left hemisphere. These
382 cortical regions are known to be involved in calculation tasks (Fehr, Code, & Herrmann, 2007;
383 Rickard et al., 2000; Rosenberg-Lee, Chang, Young, Wu, & Menon, 2011) and particularly in

384 the left hemisphere (Arsalidou & Taylor, 2011). Critically, our parietal cluster in the left
385 hemisphere ($x = -35, y = -42, z = 53$) appeared to be very close to the brain coordinate located
386 in the horizontal segment of the intraparietal sulcus ($x = -37, y = -48, z = 49$) reported by Andres
387 and colleagues (2011) and mainly involved on number magnitude processing (Dehaene, Piazza,
388 Pinel, & Cohen, 2003) or division operations (Andres et al., 2011). The similar activation of
389 brain areas typically related to arithmetic calculation and orientation averaging begs the
390 speculation of a calculation that is not specific to arithmetic. Further investigations are required
391 to investigate this speculative link.

392 Although no behavioral differences were observed between averaging in low and high variance,
393 and similar brain areas were activated, some differences in neural activity amplitude were
394 observed. The right superior frontal and left middle frontal gyri were significantly more
395 activated when the variance in the orientation of the Gabors was high than when it was low.
396 The direct comparison between high and low variance conditions also elicited an unexpected
397 cerebral activity overlapping the cerebellum (Crus I) and the inferior occipital gyrus in the left
398 hemisphere. Andres and colleagues (2011) reported a similar cluster for arithmetic operation
399 (multiplication and subtraction), but in the right hemisphere. Conversely, no cortical area
400 showed significantly more neural activation in the low variance conditions compared with the
401 high variance conditions. Thus, more neural activity was observed when estimating the mean
402 orientation of a high-variance ensemble compared to estimating the mean orientation of a low-
403 variance ensemble.

404 The additional activation that occurred in high variance relative to low variance appears to be
405 mainly driven by the 64-Gabor condition and not by the 4-Gabor condition. These results are
406 surprising to us. As mentioned in the introduction, based on a previous psychophysical study
407 (Allard & Cavanagh, 2011), we could expect voluntary averaging (i.e., 4-Gabor) to occur when
408 the elements are dissimilar (i.e., high variance), but not when they appear identical (i.e., low

409 variance) because observers may not bother averaging samples that appear identical.
410 Interestingly, however, additional activation in the right superior frontal and left middle frontal
411 gyri was observed in high variance relative to low variance for involuntary averaging (i.e., 64-
412 Gabor condition). This result was less expected, but has more impact given that most studies
413 on ensemble statistics focus on large ensembles (e.g., 64) rather than small ensembles as in
414 voluntary averaging.

415 The current finding showing additional activation in the left middle frontal gyrus with 64
416 samples in high variance relative to low variance is consistent with the hypothesis that some
417 of this additional processing is related to averaging calculation. Indeed, the middle frontal
418 gyrus from both hemispheres has been found to be involved in mental calculations involving
419 working memory, especially for complex tasks (Arsalidou & Taylor, 2011). Similarly,
420 bilateral involvement of the frontal regions in both hemispheres for the fMRI contrast [HV-64
421 > LV-64] suggested that supplementary processing were needed during high variance
422 condition (Fehr et al., 2007). Consequently, the current findings with 64 elements to average,
423 are consistent with the hypothesis that more processing relevant to the averaging calculation
424 occurs when the main source of variance was due to physical variance across elements (i.e.,
425 high variance) than when the source of variance was due to imprecision estimates by the
426 visual system (i.e., low variance). Further studies are required to test this hypothesis.

427 It is also possible that the different activation is caused by different efforts by the observer
428 due to the apparent task difficulty as the stimuli in low and high variance appear very different.
429 Some observers have reported that the task seemed more difficult when all the orientations
430 were close to vertical and others actually reported that the task was more difficult when the
431 orientations of the Gabors were dissimilar because it was more difficult to average. Thus, it is
432 possible that observers reduced their effort in low variance because they gave up more in low
433 variance (task appeared too difficult) or because they put more efforts in high variance as the

434 tasked appeared more difficult. If the observers modulated their effort based on the apparent
435 task difficulty and the effort level affects the averaging efficiency, then this would obviously
436 violate the variance-invariant processing assumption as different effective averaging
437 efficiencies would occur in low and high variance. In other words, using the equivalent noise
438 paradigm for an averaging task requires the assumption that the observer's averaging efforts
439 are not modulated by the apparent task difficulty that may differ between low and high
440 variance.

441 Note that we are not assuming that the task difficulty is the same in low and high variance; it
442 is the typical equivalent noise paradigm that relies on the assumption that the task difficulty is
443 the same in these two conditions. In high variance, the samples are all vertically oriented
444 (mean of the a priori distribution) and some orientation noise-jitter (variance of the a priori
445 distribution) is added to each sample. In absence of stimulus variance, the samples are all
446 vertically oriented and some orientation noise-jitter (due to imprecision in sample estimates
447 by the visual system, i.e., internal noise) is added to each sample. Thus, the effective stimulus
448 (i.e., samples after the internal noise is added) is supposed to be equivalent according to the
449 assumption underlying the equivalent noise paradigm (see the noise-invariant processing
450 assumption, Allard & Cavanagh, 2011, 2012; and the contrast-invariant calculation
451 assumption Pelli, 1990): samples are vertically oriented and some orientation noise-jitter is
452 added. Consequently, according to the equivalent noise paradigm, the task difficulty is
453 assumed *not* to differ between low and high variance when the a priori distribution is centered
454 on vertical. If the task difficulty differed between low and high variance conditions, then this
455 would undermine the use of the equivalent noise paradigm. In sum, the equivalent noise
456 paradigm requires to assume that the task difficult in low and high variance did not differ and
457 that observers put the same level of effort in low and high variance.

458 Nevertheless, it is possible that the effective averaging efficiency was the same in low and
459 high variance despite the fact that there was more neural activity in high variance. The
460 additional neural activity in brains areas related to arithmetic calculation may not be related to
461 the averaging process. For instance, orientation uniformity in low variance could lead to
462 greater suppression/inhibition in early visual areas and thus reduced activity is fed forward to
463 later visual areas, or higher variance could lead to richer accidental contour structure
464 activating later form-selective areas more effectively, or higher variance may produce more
465 attentionally engaging accidental stimuli soliciting more task-unrelated attention. If the
466 additional neural activity in high noise is not caused by the averaging calculation per se and it
467 does not affect indirectly the averaging process (e.g., through lateral inhibition between
468 processes or competing attentional resources), then it would be justified to assume that the
469 same effective averaging efficiency operates in low and high variance. On the other hand, if
470 the additional neural activity reflects more processing related to the involuntary averaging
471 computation, or if it reflects different efforts do to apparent task difficulty, or if it causes some
472 other process to indirectly affect the averaging computation, then it would undermine the
473 assumption that the effective averaging efficiency is the same in low and high variance.
474 Further studies are required to determine if this additional neural activity affects directly or
475 indirectly the effective averaging efficiency.

476 **Acknowledgements**

477 This research was supported by the Chair SILVERSIGHT ANR-18-CHIN-0002 and by the
478 IHU FOReSIGHT ANR-18-IAHU-01. The authors thank the participants of this study for
479 their valuable contributions. We thank the CHNO des Quinze-Vingts for enabling us to
480 perform the MRI acquisitions.

481 **Open Practices Statement**

482 The datasets generated during and/or analysed during the current study are available from the
483 corresponding author on reasonable request. The experiment was not preregistered.

484 **References**

485 Allard, R., & Cavanagh, P. (2011). Crowding in a detection task: external noise triggers change in processing
486 strategy. *Vision Research*, *51*(4), 408–416. Retrieved from
487 <http://ovidsp.ovid.com/ovidweb.cgi?T=JS&CSC=Y&NEWS=N&PAGE=fulltext&D=medl&AN=2118585>
488 5

489 Allard, R., & Cavanagh, P. (2012). Different processing strategies underlie voluntary averaging in low and high
490 noise. *Journal of Vision*, *12*(11). <https://doi.org/10.1167/12.11.6>

491 Allard, R., & Faubert, J. (2013). Zero-dimensional noise is not suitable for characterizing processing properties
492 of detection mechanisms. *Journal of Vision*, *13*(10). <https://doi.org/10.1167/13.10.25>

493 Allard, R., & Faubert, J. (2014). To characterize contrast detection, noise should be extended, not localized.
494 *Frontiers in Psychology*, *5*(749). <https://doi.org/10.3389/fpsyg.2014.00749>

495 Alvarez, G. A., & Oliva, A. (2008). The representation of simple ensemble visual features outside the focus of
496 attention: Research article. *Psychological Science*, *19*(4), 392–398. [https://doi.org/10.1111/j.1467-](https://doi.org/10.1111/j.1467-9280.2008.02098.x)
497 [9280.2008.02098.x](https://doi.org/10.1111/j.1467-9280.2008.02098.x)

498 Alvarez, G. A., & Oliva, A. (2009). Spatial ensemble statistics are efficient codes that can be represented with
499 reduced attention. *Proceedings of the National Academy of Sciences*, *106*(18), 7345–7350.
500 <https://doi.org/10.1073/pnas.0808981106>

501 Andres, M., Pelgrims, B., Michaux, N., Olivier, E., & Pesenti, M. (2011). Role of distinct parietal areas in
502 arithmetic: An fMRI-guided TMS study. *NeuroImage*. <https://doi.org/10.1016/j.neuroimage.2010.11.009>

503 Arsalidou, M., & Taylor, M. J. (2011). Is $2+2=4$? Meta-analyses of brain areas needed for numbers and
504 calculations. *NeuroImage*. <https://doi.org/10.1016/j.neuroimage.2010.10.009>

505 Baker, D. H., & Meese, T. S. (2012). Zero-dimensional noise: The best mask you never saw. *Journal of Vision*,
506 *12*(10). <https://doi.org/10.1167/12.10.20>

507 Baker, D. H., & Vilidaitė, G. (2014). Broadband noise masks suppress neural responses to narrowband stimuli.
508 *Frontiers in Psychology*, *5*(763). <https://doi.org/10.3389/fpsyg.2014.00763>

509 Baldwin, A. S., Baker, D. H., & Hess, R. F. (2016). What Do Contrast Threshold Equivalent Noise Studies
510 Actually Measure? Noise vs. Nonlinearity in Different Masking Paradigms. *PLoS ONE*, *11*(3), 1–25.
511 <https://doi.org/10.1371/journal.pone.0150942>

512 Beaudot, W. H. A., & Mullen, K. T. (2006). Orientation discrimination in human vision: Psychophysics and
513 modeling. *Vision Research*, *46*(1–2), 26–46. Retrieved from
514 [http://www.sciencedirect.com/science/article/B6T0W-4HPD3JT-](http://www.sciencedirect.com/science/article/B6T0W-4HPD3JT-1/2/d729e222ab5dd9a8a454ef8eb61f074b)
515 [1/2/d729e222ab5dd9a8a454ef8eb61f074b](http://www.sciencedirect.com/science/article/B6T0W-4HPD3JT-1/2/d729e222ab5dd9a8a454ef8eb61f074b)

516 Bocheva, N., Stefanov, S., Stefanova, M., & Genova, B. (2015). Global orientation estimation in noisy
517 conditions. *Acta Neurobiologiae Experimentalis*, *75*(4), 412–433.

518 Bronfman, Z. Z., Brezis, N., Jacobson, H., & Usher, M. (2014). We See More Than We Can Report: “Cost Free”
519 Color Phenomenality Outside Focal Attention. *Psychological Science*, *25*(7), 1394–1403.
520 <https://doi.org/10.1177/0956797614532656>

521 Chong, S. C., & Treisman, A. (2005). Statistical processing: Computing the average size in perceptual groups.
522 *Vision Research*, *45*(7), 891–900. <https://doi.org/10.1016/j.visres.2004.10.004>

523 Dakin, S. C. (2001). Information limit on the spatial integration of local orientation signals. *J. Opt. Soc. Am. A*,
524 *18*(5), 1016–1026. Retrieved from <http://josaa.osa.org/abstract.cfm?URI=josaa-18-5-1016>

525 Dakin, S. C. (2015). Seeing Statistical Regularities: Texture and Pattern Perception. *The Oxford Handbook of*
526 *Perceptual Organization*, 150–167. Retrieved from [papers://b6c7d293-c492-48a4-91d5-](papers://b6c7d293-c492-48a4-91d5-8fae456be1fa/Paper/p13817%5Cnfile:///C:/Users/Serguei/OneDrive/Documents/Papers/Seeing%20Statistical%20Regularities%20Texture%20and-2014-06-17.pdf)
527 [8fae456be1fa/Paper/p13817%5Cnfile:///C:/Users/Serguei/OneDrive/Documents/Papers/Seeing Statistical](papers://b6c7d293-c492-48a4-91d5-8fae456be1fa/Paper/p13817%5Cnfile:///C:/Users/Serguei/OneDrive/Documents/Papers/Seeing%20Statistical%20Regularities%20Texture%20and-2014-06-17.pdf)
528 [Regularities Texture and-2014-06-17.pdf](papers://b6c7d293-c492-48a4-91d5-8fae456be1fa/Paper/p13817%5Cnfile:///C:/Users/Serguei/OneDrive/Documents/Papers/Seeing%20Statistical%20Regularities%20Texture%20and-2014-06-17.pdf)

529 Dakin, S. C., Bex, P. J., Cass, J. R., & Watt, R. J. (2009). Dissociable effects of attention and crowding on
530 orientation averaging. *Journal of Vision*, *9*(11), 1–16. <https://doi.org/10.1167/9.11.28>

531 Dakin, S. C., Mareschal, I., & Bex, P. J. (2005). Local and global limitations on direction integration assessed
532 using equivalent noise analysis. *45*(UCL, Inst Ophthalmol, Dept Visual Sci, 11-43 Bath St, London EC1V
533 9EL, UK), 3027–3049. Retrieved from

534 <http://ovidsp.ovid.com/ovidweb.cgi?T=JS&PAGE=reference&D=bioba25&NEWS=N&AN=BACD20060>
535 0043651

536 Dehaene, S., Piazza, M., Pinel, P., & Cohen, L. (2003). Three parietal circuits for number processing. *Cognitive*
537 *Neuropsychology*. <https://doi.org/10.1080/02643290244000239>

538 Fehr, T., Code, C., & Herrmann, M. (2007). Common brain regions underlying different arithmetic operations as
539 revealed by conjunct fMRI-BOLD activation. *Brain Research*.
540 <https://doi.org/10.1016/j.brainres.2007.07.043>

541 Fischer, J., & Whitney, D. (2011). Object-level visual information gets through the bottleneck of crowding.
542 *Journal of Neurophysiology*, 106(3), 1389–1398. <https://doi.org/10.1152/jn.00904.2010>

543 Friston, K. J., Holmes, A. P., Worsley, K. J., Poline, J. -P, Frith, C. D., & Frackowiak, R. S. J. (1994). Statistical
544 parametric maps in functional imaging: A general linear approach. *Human Brain Mapping*.
545 <https://doi.org/10.1002/hbm.460020402>

546 Hallett, P. E. (1986). Eye movements. *Handbook of Perception and Human Performance*, 10–90.

547 Im, H. Y., & Halberda, J. (2013). The effects of sampling and internal noise on the representation of ensemble
548 average size. *Attention, Perception, and Psychophysics*, 75(2), 278–286. [https://doi.org/10.3758/s13414-](https://doi.org/10.3758/s13414-012-0399-4)
549 012-0399-4

550 Lagrené, K., Bécu, M., Seiple, W. H., Raphanel Bataille, M., Combariza, S., Paques, M., ... Arleo, A. (2019).
551 Healthy and pathological visual aging in a French follow-up cohort study. In *Investigative Ophthalmology*
552 *& Visual Science*. Vancouver, Canada.

553 Mansouri, B., Allen, H. A., Hess, R. F., Dakin, S. C., & Ehrt, O. (2004). Integration of orientation information in
554 amblyopia, 44(McGill Vis Res Unit, 687 Pine Ave W,Rm H4-14, Montreal, PQ, H3A 1A1, Canada),
555 2955–2969. Retrieved from
556 <http://ovidsp.ovid.com/ovidweb.cgi?T=JS&PAGE=reference&D=bioba24&NEWS=N&AN=BACD20050>
557 0035440

558 Mareschal, I., Bex, P. J., & Dakin, S. C. (2008). Local motion processing limits fine direction discrimination in
559 the periphery, 48(UCL, UCL Inst Ophthalmol, Bath St, London EC1V 9EL, UK), 1719–1725. Retrieved
560 from
561 <http://ovidsp.ovid.com/ovidweb.cgi?T=JS&PAGE=reference&D=bioba27&NEWS=N&AN=BACD20080>
562 0479314

563 Parkes, L., Lund, J., Angelucci, A., Solomon, J. A., & Morgan, M. (2001). Compulsory averaging of crowded
564 orientation signals in human vision. *Nature Neuroscience*, 4(7), 739–744. <https://doi.org/10.1038/89532>

565 Pelli, D. G. (1990). The quantum efficiency of vision. In C. Blakemore (Ed.), *Visual coding and efficiency* (pp.
566 3–24). Cambridge: Cambridge University Press.

567 Pylyshyn, Z. W., & Storm, R. W. (1988). Tracking multiple independent targets: evidence for a parallel tracking
568 mechanism. *Spatial Vision*, 3(3), 179–197. <https://doi.org/10.1163/156856888X00122>

569 Rickard, T. C., Romero, S. G., Basso, G., Wharton, C., Flitman, S., & Grafman, J. (2000). The calculating brain:
570 An fMRI study. *Neuropsychologia*. [https://doi.org/10.1016/S0028-3932\(99\)00068-8](https://doi.org/10.1016/S0028-3932(99)00068-8)

571 Rosenberg-Lee, M., Chang, T. T., Young, C. B., Wu, S., & Menon, V. (2011). Functional dissociations between
572 four basic arithmetic operations in the human posterior parietal cortex: A cytoarchitectonic mapping study.
573 *Neuropsychologia*. <https://doi.org/10.1016/j.neuropsychologia.2011.04.035>

574 Tibber, M. S., Anderson, E. J., Bobin, T., Carlin, P., Shergill, S. S., & Dakin, S. C. (2015). Local and global
575 limits on visual processing in schizophrenia. *PLoS ONE*, 10(2).
576 <https://doi.org/10.1371/journal.pone.0117951>

577 Treisman, A. M., & Gelade, G. (1980). A feature-integration theory of attention. *Cognitive Psychology*, 12(1),
578 97–136.

579 Whitney, D., & Yamanashi Leib, A. (2018). Ensemble Perception. *Annual Review of Psychology*, 69(1),
580 annurev-psych-010416-044232. <https://doi.org/10.1146/annurev-psych-010416-044232>

581

582

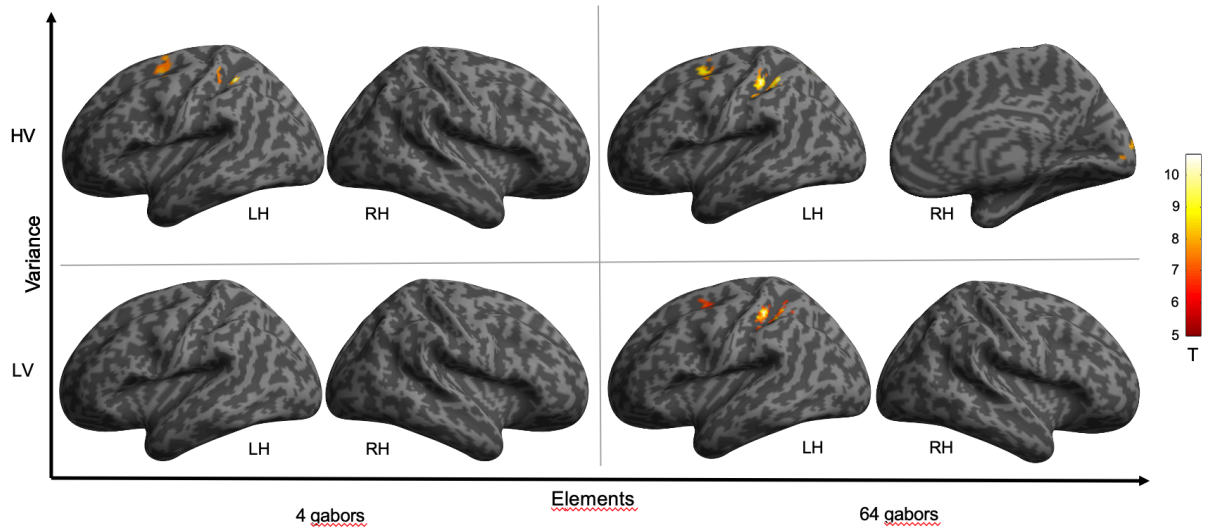
583 **Supplementary information**

fMRI contrasts		H	BA	k	x	y	z	t
[LV-4 > Fix]	<i>No significant activation</i>							
[HV-4 > Fix]	Superior Parietal Gyrus	L	7	59	-35	-42	53	9.51
	[Postcentral Gyrus]		1		-40	-35	50	5.53
	Middle Frontal Gyrus	L	6	103	-27	1	63	6.96
	[Middle Frontal Gyrus]				-25	-5	53	6.36
	[Superior Frontal Gyrus]				-17	-2	50	6.27
[LV-64 > Fix]	Supramarginal Gyrus	L	1	160	-42	-35	48	11.54
	[Superior Parietal Gyrus]		7		-35	-42	53	8.18
	[Superior Parietal Gyrus]				-20	-60	58	5.85
	Middle Frontal Gyrus	L	6	52	-32	-2	58	6.28
					-22	-2	48	6.12
[HV-64 > Fix]	Supramarginal Gyrus	L	1	231	-40	-35	45	9.53
	[Superior Parietal Gyrus]		7		-35	-42	53	8.88
	[Superior Parietal Gyrus]				-22	-55	48	7.08
	Superior Frontal Gyrus	L	6	145	-20	1	50	8.04
	[Middle Frontal Gyrus]				-30	-2	58	7.00
	Middle Occipital Gyrus	R	18	50	13	-95	13	6.32
	[Lingual Gyrus]		17		16	-87	0	5.58

584 **Table S1. Cerebral regions exhibiting an effect for the number of elements related to the variance contents**
585 **(low-variance with 4 elements: LV-4, high-variance with 4 elements: HV-4, low-variance with 64**
586 **elements: LV-64 and high-variance with 64 elements: HV-64) related to fixation (Fix). The statistical**
587 **threshold for cluster was defined as $p < 0.05$ FWE corrected for multiple comparisons with an extent voxel**
588 **threshold defined as 20 voxels. Only regions revealing significant differences between conditions were**
589 **included. For each cluster, the region showing the maximum t-value was listed first, followed by the other**
590 **regions in the cluster [in square brackets]. Montreal Neurological Institute (MNI) coordinates (x, y, z) of**

591 the peak and number of voxels (k) of clusters are also shown. H = hemisphere; R = right hemisphere; L =
592 left hemisphere; BA = Brodmann area.

593



594

595 **Figure S1. Cerebral regions whose activity was elicited by the fMRI contrasts [LV-4 > Fix], [HV-4 > Fix],**
596 **[LV-64 > Fix] and [HV-64 > Fix] projected onto 3D anatomical templates ($p < 0.05$ FWE-corrected at**
597 **cluster level, $k=20$; LV = low-variance, HV = high-variance, Fix = fixation LH = left hemisphere, RH =**
598 **right hemisphere).**